MDPI

Article

Asperflaloids A and B from *Aspergillus flavipes* DZ-3, an Endophytic Fungus of *Eucommia ulmoides* Oliver

Wan Liu [1], Yu Liu [1], Fan Yang [1], Shouye Han [1], Jia Zhang [1], Hui Yang [1,*], Zhongbin Cheng [1,2,*] and Qin Li [1,2,*]

[1] School of Pharmacy, Henan University, Kaifeng 475004, China; 18737806806@163.com (W.L.); liuyu5230710@163.com (Y.L.); Y18992588130@126.com (F.Y.); hanshouye123@163.com (S.H.); z919395@126.com (J.Z.)

[2] Eucommia Ulmoides Cultivation and Utilization of Henan Engineering Laboratory, Kaifeng 475004, China

[*] Correspondence: 10200097@vip.henu.edu.cn (H.Y.); chengzhongbin@henu.edu.cn (Z.C.); liqin@henu.edu.cn (Q.L.); Tel.: +86-371-2388-3849 (Q.L.)

Abstract: The fungus strain DZ-3 was isolated from twigs of the well-known medicinal plant *Eucommia ulmoides* Oliver and identified as *Aspergillus flavipes*. Two new alkaloids, named asperflaloids A and B (**1** and **2**), together with 10 known compounds (**3–12**) were obtained from the EtOAc extract of the strain. Interestingly, the alkaloids **1–4** with different frameworks are characterized by the presence of the same anthranilic acid residue. The structures were established by detailed analyses of the spectroscopic data. The absolute configuration of asperflaloids A and B was resolved by quantum chemistry calculation. All compounds were screened for their inhibitions against α-glucosidase and the antioxidant capacities. The results were that compound **3** had an IC_{50} value of 750.8 μM toward α-glucosidase, and the phenol compounds **7** and **8** exhibited potent antioxidant capacities with IC_{50} values 14.4 and 27.1 μM respectively.

Keywords: *Aspergillus flavipes* DZ-3; asperflaloids A and B; structural identification; bioactivity

1. Introduction

Fungi are widespread in natural environments and have conquered almost all ecological niches. Moreover, fungi produce many structurally intriguing molecules, many of which exhibit promising pharmacological properties, including the famous antibiotics penicillin and cephalosporin C [1,2]. *Aspergillus*, a genus of filamentous fungi, is noted for its medical and commercial significance. Species in *Aspergillus* have been proved to be prolific and are considered as an important source of chemical leads with hopeful biological activities [3,4]. Among the *Aspergillus* species, *Aspergillus flavipes* was an outstanding member; recent chemical research of the species resulted in the production of plenty of molecules with new structures and obvious biological activities, such as structurally complex merocytochalasans [5–7], lumazine peptides possessing significant antibacterial and NF-κB inhibitory activities [8], unusual chlorinated PKS-NRPS hybrid metabolites bearing potent pancreatic lipase inhibitory activity [9], and rare prenylated phenylbutyrolactones [10].

In our continuous efforts to search for bioactive natural products from fungus [11–15], an endophytic fungus *Aspergillus flavipes* DZ-3 was isolated from the twigs of the medicinal plant *Eucommia ulmoides* Oliver. The ^{1}H-NMR spectrum and thin layer chromatography examination using the modified Dragendorff's reagent of the EtOAc extract indicated the presence of aromatic alkaloids. Extensive chromatographic separation of the large-scale fermentation were carried out, which resulted in the isolation of 12 compounds **1–12** (Figure 1), including two new alkaloids. All compounds were screened for their inhibitions against α-glucosidase and the antioxidant capacities. Herein, the isolation, structure determination, and bioactivities of compounds **1–12** are described.
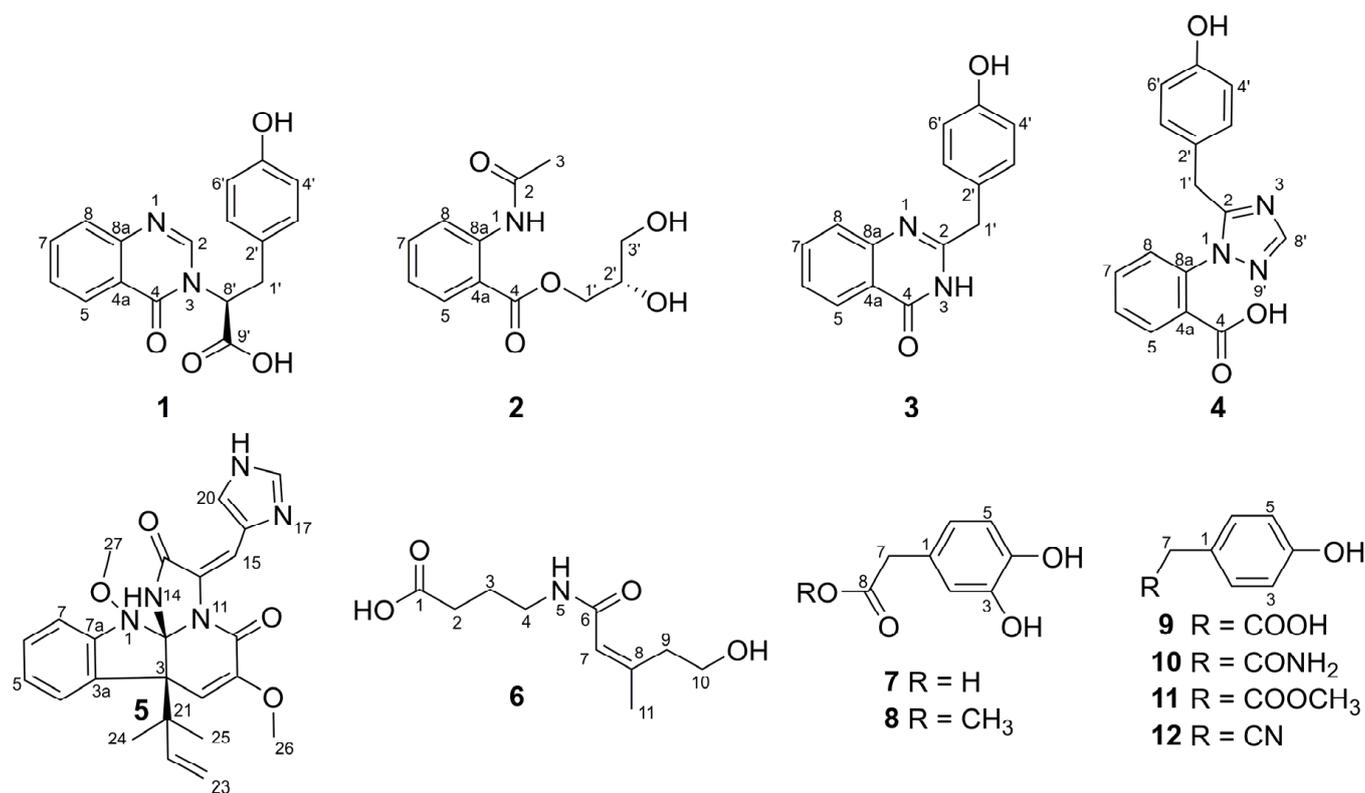
Figure 1. Structures of compounds **1–12** from *Aspergillus flavipes* DZ-3.

2. Results

Asperflaloid A (**1**) has a molecular formula of $C_{17}H_{14}N_2O_4$ (309.0879 [M − H]⁻, calcd for $C_{17}H_{13}N_2O_4^-$, 309.0881) as determined by the HRESIMS and NMR data (Table 1, Figures S1–S6, S33), bearing 12 degrees of unsaturation. The ¹H-NMR spectrum showed an ABCD aromatic spin system for an ortho-disubstituted benzene ring [δ_H 7.62 (1H, d, *J* = 8.1 Hz); 7.80 (1H, dd, *J* = 8.1, 7.5 Hz); 7.54 (1H, dd, *J* = 7.9, 7.5 Hz); 8.20 (1H, d, *J* = 7.9 Hz)]; and an AABB aromatic spin system for a para-disubstituted benzene ring [δ_H 6.93, (2H, d, *J* = 8.3 Hz); 6.60 (2H, d, *J* = 8.3 Hz)]. Comprehensive analyses of 2D NMR (COSY, HSQC, HMBC) data revealed that the structure of **1** consists of a quinazoline moiety and a phenylpropionic acid moiety (Figure 2). The COSY relationships connected the protons from H-5 (δ_H 8.20) to H-8 (δ_H 7.62), while the HMBC correlations between H-5 and C-4 (δ_C 162.3) and from H-2 (δ_H 7.94) to C-8a (δ_C 148.5) and C-4 assigned the quinazoline ring. The phenylpropionic acid moiety was established by ¹H-¹H COSY relationship between H₂-1′ (δ_H 3.44, 3.53) and H-8′ (δ_H 5.40), and HMBC correlations from H₂-1′ to C-2′ (δ_C 128.4), C-3′ (δ_C 131.1), C-7′ (δ_C 131.1), in association with HMBC correlation from H-8′ to the carboxylic carbon C-9′ (δ_C 172.2). The above two moieties were connected by a C-N bond supported by the HMBC correlations from H-8′ to C-2 (δ_C 148.6) and C-4. Thus, the gross structure of **1** was assigned as depicted. The absolute configuration of the only chiral center C-8′ (δ_C 62.3) in **1** was determined by comparisons of experimental electronic circular dichroism (ECD) with calculated ECD spectra (Figure 3, Figure S35). The calculations of the ECD spectrum of (8′*S*)-**1** and its enantiomer (8′*R*)-**1** were performed using b3lyp/6–31+g(d,p) optimized geometries after conformational searches via the MMFF94S force field at the b3lyp/6–31+g(d,p) level in methanol. The experimental ECD spectrum of **1** showed an ECD curve with Cotton effects around 228 (−) and 270 (−) nm, respectively (Figure 3). The calculated ECD spectrum for (8′*S*)-1 showed a similar ECD curve with Cotton effects at 231 nm (−) and 290 (−) nm, allowing the assignment of the 8′*S* configuration for **1**.

Table 1. ^{1}H (400 MHz) and ^{13}C-NMR (100 MHz) data of **1** and **2** (In methanol-d_4).

No.	**1**		**2**	
	δ_H (*J* in Hz)	δ_C	δ_H (*J* in Hz)	δ_C
2	7.94, s	148.6		171.6
3			2.21, s	24.9
4		162.3		169.1
4a		122.7		118.1
5	8.20, d (7.9)	127.5	8.11, dd (8.0, 1.6)	132.2
6	7.54, dd (7.9, 7.5)	128.6	7.18, dd (8.0, 7.9, 1.0)	124.3
7	7.80, dd (8.1, 7.5)	135.9	7.57, dd (8.3, 7.9, 1.6)	135.2
8	7.62, d (8.1)	127.8	8.45, dd (8.3, 1.0)	122.1
8a		148.5		141.8
1'	3.44, dd (14.4, 4.8); 3.53, dd (14.4, 10.9)	35.6	4.45, dd (11.4, 4.1); 4.34, dd (11.4, 6.3)	67.5
2'		128.4	3.99, m	71.0
3'	6.93, d (8.3)	131.1	3.65, d (5.7)	64.0
4'	6.60, d (8.3)	116.5		
5'		157.5		
6'	6.60, d (8.3)	116.5		
7'	6.93, d (8.3)	131.1		
8'	5.40, dd (10.9, 4.8)	62.3		
9'		172.2		
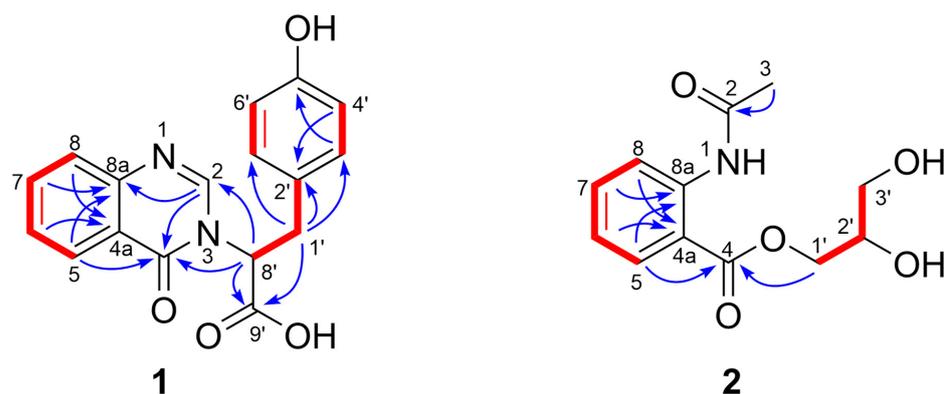
Figure 2. ^{1}H-^{1}H COSY (━) and HMBC (⌣) correlations of **1** and **2**.
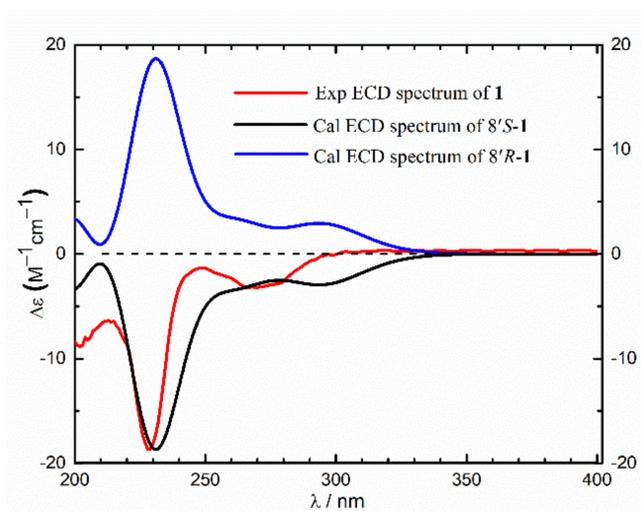
Figure 3. Experimental and calculated electronic circular dichroism (ECD) spectra of **1** in MeOH (σ = 0.3, UV correction = −5 nm).

The molecular formula of compound **2** was determined to be $C_{12}H_{15}NO_5$ (254.1024 $[M + H]^+$, calcd for $C_{12}H_{16}NO_5^+$, 254.1023) by the HRESIMS and NMR data (Table 1, Figures S7–S12, S34), suggesting six degrees of unsaturation. The ^1H-NMR spectrum exhibited the resonances of four aromatic protons [δ_H 8.11 (1H, dd, J = 8.1, 1.6 Hz); 7.18 (1H, dd, J = 8.0, 7.9, 1.0 Hz); 7.57 (1H, dd, J = 8.3, 7.9, 1.6 Hz); 8.45 (1H, dd, J = 8.3, 1.0 Hz)] for an ABCD aromatic spin system, two oxygenated methylenes [δ_H 4.45 (1H, dd, J = 11.4, 4.1 Hz), 4.34 (1H, dd, J = 11.4, 6.3 Hz); 3.65 (2H, d, J = 5.7 Hz)], an oxygenated methine [δ_H 3.99 (1H, m)], and a methyl [δ_H 2.21 (3H, s)]. The ^{13}C-NMR and HSQC spectra resolved six aromatic carbons for a benzene ring (δ_C 141.8, 118.1, 132.2, 124.3, 135.2, 122.1), two carbonyl carbons (δ_C 169.1, 171.6) for ester/amide groups, two oxygenated methylene carbons (δ_C 67.5, 64.0), and an oxygenated methine carbon (δ_C 71.0). The benzene ring and the two carbonyl groups covered all six degrees of unsaturation, suggesting that no additional ring exists in the structure. The ^1H-^1H COSY correlations from H-5 (δ_H 8.11) to H-8 supported the presence of an *ortho*-disubstituted benzene ring. The COSY relationships from H_2-1′ (δ_H 4.45, 4.34) to H_2-3′ (δ_H 3.65) via H-2′ combined with the HMBC correlation from H-1′ and H-5 to C-4 located a 2,3-dihydroxypropyl formate moiety at C-4a. The substituent group at C-8a was established to be an acetyl amino group by the HMBC correlation from H-5 to C-4 in association with the HRESIMS data, which was also supported by the chemical shifts of C-8a. The gross structure of **2** was thus determined as shown in Figure 1. In order to resolve the absolute configuration of the only chiral center C-2′ in **2**, theoretical specific rotations of the model molecules *S*/*R*-**2** were calculated at the b3lyp/6-31+g(d) level using methanol as solvent. The results were that the theoretical specific rotation of *S*-**2** (*S*-**2**: $[\alpha]_D^{20}$ +147; *R*-**2**: $[\alpha]_D^{20}$ −147) had the same sign as the experimental data of **2** ($[\alpha]_D^{20}$ +270), indicating a 2′*S*-configuration for **2**. A comparison of the specific rotations of **2**, (*S*)-1-benzoyloxypropane-2,3-diol $[\alpha]_D^{20}$ +15.8), and (*R*)-1-benzoyloxypropane-2,3-diol ($[\alpha]_D^{20}$ −15.9) supported the 2′*S*-configuration of **2** (Figure 4) [16]. Compound **2** was given the trivial name asperflaloid B.
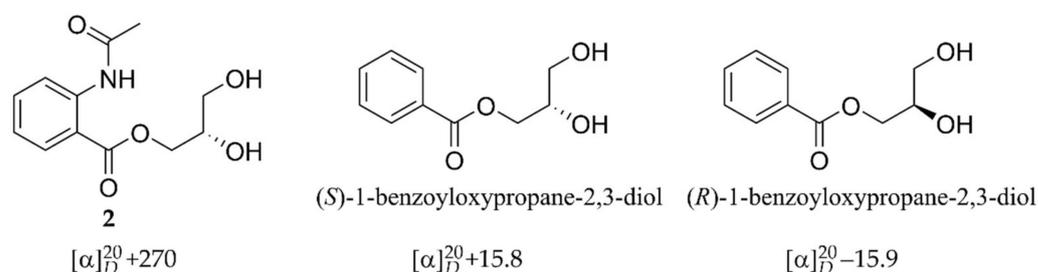

Figure 4. Structures and specific rotations of **2** and (*S*/*R*)-1-benzoyloxypropane-2,3-diol.

The remaining compounds were identical to 2-(4-hydroxybenzyl)quinazolin-4(3*H*)-one (**3**) [17], penipanoid A (**4**) [18], oxaline (**5**) [19], fuscoatramide (**6**) [20], 3,4-dihydroxybenzeneacetic acid (**7**) [21], 3,4-dihydroxyphenylacetic acid methyl ester (**8**) [21], phenylacetic acid (**9**) [22], 4-hydroxybenzeneacetamide (**10**) [23], 4-hydroxy phenylacetic acid methyl ester (**11**) [24], and 4-hydroxyphenylacetonitrile (**12**) [23] based on comparisons of their NMR data (Figures S13–S32) and specific rotations with those reported in the literature.

All compounds were tested for their α-glucosidase inhibitory activities and antioxidant capacities (Table 2). We found that compound **3** inhibited α-glucosidase with an IC_{50} value of 750.8 μM and was more active than the positive control acarbose (1.33 mM). Compounds **7** and **8** exhibited strong antioxidant capacities with IC_{50} values 14.4 and 27.1 μM, respectively, which were comparable to that of vitamin C (26.7 μM). Compound **10** exhibited weak antioxidant capacity with an IC_{50} value 339.3 μM. Other compounds exhibited negligible activity at the concentration of 1 mM.

Table 2. The α-glucosidase inhibitory and antioxidant activities of compounds **1–12**.

Compounds	α-Glucosidase Inhibitory	Antioxidant	
	IC$_{50}$ (μM)	% Inhibition (500 μM)	IC$_{50}$ (μM)
1	−	<50	−
2	−	<50	−
3	750.8	<50	−
4	−	<50	−
5	−	<50	−
6	−	<50	−
7	−	96.6	14.4
8	−	92	27.1
9	−	<50	−
10	−	64.9	339.3
11	−	<50	−
12	−	<50	−
Acarbose [a]	1330		
Vitamin C [a]		96.4	26.7

− means no activity; [a] positive control.

3. Materials and Methods

3.1. General Experimental Procedure

Specific rotations were measured by an SGW-1 automatic polarimeter (Shanghai Jing Ke Industrial Co., Ltd., Shanghai, China). ECD spectra were measured on an Aviv Model 420SF spectropolarimeter (Aviv Biomedical Inc., Lakewood, NJ, USA). The NMR spectra were recorded on a Bruker Avance III HD-400 NMR spectrometer. HRESIMS spectra were obtained on a Waters Xevo G2 Q-TOF spectrometer fitted with an ESI source. Semi-preparative high-performance liquid chromatography (HPLC) was undertaken on a Shimadzu LC-6AD pump (Shimadzu Co., Kyoto, Japan) using a UV detector, and a YMC-Pack ODS-A HPLC column (semipreparative, 250 × 10 mm, S-5 μm, 12 nm, YMC Co., Ltd., Kyoto, Japan) was used for separation.

3.2. Fungal Strain and Identification

Fungus DZ-3 was isolated from branches of *Eucommia ulmoides* Oliver. The strain was identified as *Aspergillus flavipes* based on microscopic examination and by internal transcribed spacer (ITS) sequencing. The ITS sequence has been deposited in GenBank (http://www.ncbi.nlm.nih.gov, accessed on 13 May 2021) with the accession number MZ148624. The strain DZ-3 (henuyxydz-3) was deposited at the School of pharmacy, Henan University.

3.3. Fermentation, Extraction, and Isolation

The fermentation was carried out in 30 Fernbach flasks (500 mL), each containing 70 g of rice. Distilled water (90 mL) was added to each flask, and the contents were soaked for 3 h before autoclaving at 15 psi for 30 min. After cooling to room temperature, each flask was inoculated with 3.0 mL of the spore inoculum and incubated at room temperature for 30 days. The fermented material was extracted successively with EtOAc (3 × 4000 mL). After evaporation under vacuum, the EtOAc extract (1.6 g) was subjected to a middle chromatogram isolated gel (MCI) with MeOH/H$_2$O (10:90 → 100:0) as eluent to obtain 7 fractions (F1 to F7). Fraction F2 was further chromatographed over ODS silica gel CC eluted with MeOH/H$_2$O (30:70 → 100:0) to afford ten subfractions (SF2a–SF2j). SF2a was separated on a semipreparative reversed-phase (RP) HPLC column using MeCN/H$_2$O = 20:80 (3 mL/min) to give **6** (t$_R$ = 7.0 min, 4.7 mg). SF2c was purified by HPLC using MeCN/H$_2$O = 21:79 (3 mL/min) as eluent to give **2** (t$_R$ = 14.5 min, 1.5 mg). SF2e was subjected by HPLC using MeCN/H$_2$O = 34:66 (3 mL/min) to give **4** (t$_R$ = 10.3 min, 4.3 mg). SF2h was purified by HPLC using MeCN/H$_2$O = 50.5:49.5 (3 mL/min) as a mobile

phase to give **5** (t$_R$ = 6.2 min, 9.8 mg). Fraction F3 was further chromatographed over ODS silica gel CC eluted with MeOH/H$_2$O (30:70 → 90:10) to afford five subfractions (SF3a–SF3e). SF3a was separated on HPLC using MeCN/H$_2$O = 14:86 (3 mL/min) as eluent to afford **7** (t$_R$ = 10.7 min, 12.0 mg), **8** (t$_R$ = 31.5 min, 6.5 mg), **9** (t$_R$ = 17.6 min, 12.9 mg), **10** (t$_R$ = 7.7 min, 16.1 mg) and **12** (t$_R$ = 32.9 min, 3.8 mg). SF3b was further purified on HPLC using MeCN/H$_2$O = 20:80 (3 mL/min) as a mobile phase to obtain **1** (t$_R$ = 40.5 min, 29.4 mg) and **11** (t$_R$ = 34.7 min, 14.1 mg). Compound **3** was precipitated from SF3c.

Asperflaloid A (**1**): Brown oil; $[\alpha]_D^{20}$ –47 (c 0.08, MeOH); UV (MeOH) λmax 225 nm, 271 nm, 302 nm; ^{1}H and ^{13}C-NMR data, see Table 1; HRESIMS m/z 309.0879 [M − H]$^-$ (calcd for C$_{17}$H$_{13}$N$_2$O$_4^-$, 309.0881).

Asperflaloid B (**2**): Colorless oil; $[\alpha]_D^{20}$ +270 (c 0.035, MeOH); UV (MeOH) λmax 221 nm, 249 nm, 304 nm; ^{1}H and ^{13}C-NMR data, see Table 1; HRESIMS m/z 254.1024 [M + H]$^+$ (calcd for C$_{12}$H$_{16}$NO$_5^+$, 254.1023).

3.4. α-Glucosidase Assay

The α-glucosidase inhibitory effect was assessed as described in our recently published paper [25].

3.5. Antioxidant Activity

The DPPH scavenging was assayed according to the reported method [26]. The DPPH radical scavenging test was performed in 96-well microplates. Samples (compounds **1**–**12**) were added to 180 μL (150 μmol/L) DPPH solution in EtOH at 20 μL solutions of different concentrations between 10 and 500 μM. After 30 min of light avoidance, absorbance at 517 nm using a microplate reader (Tecan Trading AG, Männedorf, Switzerland) was measured and the percentage of activity was calculated. All assays were performed in three replicates, and vitamin C was used as a positive control.

3.6. Computational Details

ECD calculations. Conformational analyses were carried out via random searching in the Sybyl-X 2.0 using the MMFF94S force field with an energy cutoff of 2.5 kcal/mol [27]. The results showed the three lowest energy conformers for *R*-**1.** The conformers were re-optimized using DFT at the b3lyp/6-31+g(d,p) level in methanol by the GAUSSIAN 09 program [28]. The energies, oscillator strengths, and rotational strengths (velocity) of the first 30 electronic excitations were calculated using the TDDFT methodology at the b3lyp/6-31+g(d,p) level in methanol. The ECD spectra were simulated by the overlapping Gaussian function (half the bandwidth at 1/e peak height, σ = 0.3, UV correction = −5 nm) [29]. To get the final spectra, the simulated spectra of the conformers were averaged according to the Boltzmann distribution theory and their relative Gibbs free energy (ΔG), theoretical ECD spectrum of the corresponding enantiomer *S*-**1** was obtained by inverse of the ECD spectrum of *R*-**1**, respectively. By comparing the experiment spectrum with the calculated ECD spectra, the absolute configuration of the chiral center C-8′ in **1** was resolved to be *S*.

Specific rotation calculations. Conformational analyses were carried out via random searching in the Sybyl-X 2.0 using the MMFF94S force field with an energy cutoff of 2.0 kcal/mol. The results showed the three lowest energy conformers for *R*-**2**. The conformers were re-optimized using DFT at the b3lyp/6-31+g(d,p) level in methanol by the GAUSSIAN 09 program. The specific rotations for each conformer were calculated using the TDDFT methodology at the b3lyp/6-31+g(d) level in methanol. The specific rotations obtained for the conformers were averaged according to the Boltzmann distribution theory and their relative Gibbs free energy (ΔG) to give the specific rotation of *R*-**2**, the specific rotation of *S*-**2** was theoretically determined to be the opposite value of *R*-**2**. By comparing the experiment data ($[\alpha]_D^{20}$ +270) with the calculated data (*R*-**2**: $[\alpha]_D^{20}$ −147; *S*-**2**: $[\alpha]_D^{20}$ +147), the absolute configuration of the chiral center C-2′ in **2** was resolved to be *S*.

4. Conclusions

Chemical investigation of the EtOAc extract of an endophytic fungus *Aspergillus flavipes* DZ-3 led to the isolation of two new alkaloids, named asperflaloids A and B (**1**–**2**), and 10 known compounds (**3**–**12**). The structures were established by extensive analyses of spectroscopic data (1D and 2D NMR, HRESIMS) and quantum chemistry calculation. Compound **3** exhibited inhibitory effect toward α-glucosidase with an IC_{50} value of 750.8 μM and was more active than the positive control acarbose (1.33 mM). Compounds **7** and **8** exhibited remarkable antioxidant capacities with IC_{50} values of 14.4 and 27.1 μM, respectively, which were comparable to that of the positive control vitamin C (26.7 μM).

Supplementary Materials: The following are available online. Figures S1–S34, S35 and S36: ^{1}H, ^{13}C-NMR, HSQC, ^{1}H-^{1}H COSY, HMBC, NOESY, and HRESIMS spectra of new compounds **1** and **2**, ^{1}H and ^{13}C-NMR spectra of compounds **3**–**12**, and computational details for ECD calculations of **1** and specific rotation calculations of **2**.

Author Contributions: W.L. and Y.L. isolated the compounds and elucidated the structures; F.Y. and J.Z. tested the bioactivity assay; H.Y. and S.H. isolated and identified the fungus and conducted the solid fermentation of the fungus; H.Y. calculated the ECD data. Q.L. and Z.C. designed the experiment and edited the manuscript. All authors have read and agreed to the published version of the manuscript.

Data Availability Statement: All data and figures in this study are openly available.

Conflicts of Interest: The authors declare no conflict of interest.

Sample Availability: Samples of the compounds **1**–**12** are available from the authors.

References

1. Spiteller, P. Chemical ecology of fungi. *Nat. Prod. Rep.* **2015**, *32*, 971–993. [CrossRef]
2. Rateb, M.E.; Ebel, R. Secondary metabolites of fungi from marine habitats. *Nat. Prod. Rep.* **2011**, *28*, 290–344. [CrossRef] [PubMed]
3. El-hawary, S.S.; Moawad, A.S.; Bahr, H.S.; Abdelmohsen, U.R.; Mohammed, R. Natural product diversity from the endophytic fungi of the genus *Aspergillus*. *RSC Adv.* **2020**, *10*, 22058–22079. [CrossRef]
4. Sanchez, J.F.; Somoza, A.D.; Keller, N.P.; Wang, C.C.C. Advances in *Aspergillus* secondary metabolite research in the post-genomic era. *Nat. Prod. Rep.* **2012**, *29*, 351–371. [CrossRef]
5. Zhu, H.C.; Chen, C.M.; Tong, Q.Y.; Yang, J.; Wei, G.Z.; Xue, Y.B.; Wang, J.P.; Luo, Z.W.; Zhang, Y.H. Asperflavipine A: A cytochalasan heterotetramer uniquely defined by a highly complex tetradecacyclic ring system from *Aspergillus flavipes* QCS12. *Angew. Chem. Int. Edit.* **2017**, *56*, 5242–5246. [CrossRef] [PubMed]
6. Zhu, H.C.; Chen, C.M.; Tong, Q.Y.; Li, X.N.; Yang, J.; Xue, Y.B.; Luo, Z.W.; Wang, J.P.; Yao, G.M.; Zhang, Y.H. Epicochalasines A and B: Two bioactive merocytochalasans bearing caged epicoccine dimer units from *Aspergillus flavipes*. *Angew. Chem. Int. Edit.* **2016**, *55*, 3486–3490. [CrossRef]
7. Zhang, X.T.; Yang, L.; Wang, W.J.; Wu, Z.D.; Wang, J.P.; Sun, W.G.; Li, X.N.; Chen, C.M.; Zhu, H.C.; Zhang, Y.H. Flavipesines A and B and asperchalasines E-H: Cytochalasans and merocytochalasans from *Aspergillus flavipes*. *J. Nat. Prod.* **2019**, *82*, 2994–3001. [CrossRef]
8. Wang, C.; Wu, X.H.; Bai, H.L.; Zaman, K.; Hou, S.B.; Saito, J.; Wongwiwatthananukit, S.; Kim, K.S.; Cao, S.G. Antibacterial and NF-kappa B inhibitory lumazine peptides, aspochalasin, gamma-butyrolactone derivatives, and cyclic peptides from a hawaiian *Aspergillus flavipes*. *J. Nat. Prod.* **2020**, *83*, 2233–2240. [CrossRef]
9. Jiao, W.H.; Xu, Q.H.; Ge, G.B.; Shang, R.Y.; Zhu, H.R.; Liu, H.Y.; Cui, J.; Sun, F.; Lin, H.W. Flavipesides A–C, PKS-NRPS hybrids as pancreatic lipase inhibitors from a marine sponge symbiotic fungus *Aspergillus flavipes* 164013. *Org. Lett.* **2020**, *22*, 1825–1829. [CrossRef]
10. Machado, F.P.; Kumla, D.; Pereira, J.A.; Sousa, E.; Dethoup, T.; Freitas-Silva, J.; Costa, P.M.; Mistry, S.; Silva, A.M.S.; Kijjoa, A. Prenylated phenylbutyrolactones from cultures of a marine sponge-associated fungus *Aspergillus flavipes* KUFA1152. *Phytochemistry* **2021**, *185*, 112709. [CrossRef]
11. Li, Q.; Xu, W.; Fan, R.; Zhang, J.; Li, Y.; Wang, X.; Han, S.; Liu, W.; Pan, M.; Cheng, Z. Penithoketone and penithochromones A-L, polyketides from the deep-sea-derived fungus *Penicillium thomii* YPGA3. *J. Nat. Prod.* **2020**, *83*, 2679–2685. [CrossRef]

12. Cheng, Z.; Li, Y.; Xu, W.; Liu, W.; Liu, L.; Zhu, D.; Kang, Y.; Luo, Z.; Li, Q. Three new cyclopiane-type diterpenes from a deep-sea derived fungus *Penicillium* sp. YPGA11 and their effects against human esophageal carcinoma cells. *Bioorg. Chem.* **2019**, *91*, 103129. [CrossRef]

13. Cheng, Z.; Li, Y.; Liu, W.; Liu, L.; Liu, J.; Yuan, W.; Luo, Z.; Xu, W.; Li, Q. Butenolide derivatives with α-glucosidase inhibitions from the deep-sea-derived fungus *Aspergillus terreus* YPGA10. *Mar. Drugs* **2019**, *17*, 332. [CrossRef] [PubMed]

14. Li, Y.; Liu, W.; Han, S.; Zhang, J.; Xu, W.; Li, Q.; Cheng, Z. Penitholabene, a rare 19-nor labdane-type diterpenoid from the deep-sea-derived fungus *Penicillium thomii* YPGA3. *Fitoterapia* **2020**, *146*, 104691. [CrossRef] [PubMed]

15. Li, Y.L.; Liu, W.; Xu, W.; Zeng, X.; Cheng, Z.B.; Li, Q. Aspterrics A and B, new sesquiterpenes from deep sea-derived fungus *Aspergillus terreus* YPGA10. *Rec. Nat. Prod.* **2020**, *14*, 18–22. [CrossRef]

16. Casati, S.; Ciuffreda, P.; Santaniello, E. Synthesis of enantiomerically pure (*R*)-and (*S*)-1-benzoyloxypropane-2,3-diol and revision of the stereochemical outcome of the *Candida antarctica* lipase-catalyzed benzoylation of glycerol. *Tetrahedron Asymmetry* **2011**, *22*, 658–661. [CrossRef]

17. Ma, C.; Li, Y.; Niu, S.; Zhang, H.; Liu, X.Z.; Che, Y.S. N-hydroxypyridones, phenylhydrazones, and a quinazolinone from *Isaria farinosa*. *J. Nat. Prod.* **2011**, *74*, 32–37. [CrossRef]

18. Li, C.S.; An, C.Y.; Li, X.M.; Gao, S.S.; Cui, C.M.; Sun, H.F.; Wang, B.G. Triazole and dihydroimidazole alkaloids from the marine sediment-derived fungus *Penicillium paneum* SD-44. *J. Nat. Prod.* **2011**, *74*, 1331–1334. [CrossRef]

19. Li, Y.; Li, X.F.; Kim, D.S.; Choi, H.O.; Son, B.W. Indolyl alkaloid derivatives, N_b-acetyltryptamine and oxaline from a marine-derived fungus. *Arch. Pharm. Res.* **2003**, *26*, 21–23. [CrossRef]

20. Biren, K.J.; James, B.G.; Donald, T.W. Bioactive natural products from a sclerotium-colonizing isolate of *Humicola fuscoatra*. *J. Nat. Prod.* **2002**, *65*, 1734–1737.

21. Li, L.Y.; Yi, J.L.; Cai, J.; Zhou, X.M.; Chen, L.; Zhuo, X.; Lai, X.Y. Two new bioactive secondary metabolites from the endophytic fungus *Talaromyces assiutensis* JTY2. *Nat. Prod. Res.* **2021**. [CrossRef] [PubMed]

22. Milne, J.E.; Storz, T.; Colyer, J.T.; Thiel, O.R.; Seran, M.D.; Larsen, R.D.; Murry, J.A. Iodide-catalyzed reductions: Development of a synthesis of phenylacetic acids. *J. Org. Chem.* **2011**, *76*, 9519–9524. [CrossRef]

23. Agerbirk, N.; Warwick, S.I.; Hansen, P.R.; Olsen, C.E. *Sinapis* phylogeny and evolution of glucosinolates and specific nitrile degrading enzymes. *Phytochemistry* **2008**, *69*, 2937–2949. [CrossRef] [PubMed]

24. Bose, D.S.; Narsaiah, A.V. An efficient asymmetric synthesis of (*S*)-atenolol: Using hydrolytic kinetic resolution. *Bioorg. Med. Chem.* **2005**, *13*, 627–630. [CrossRef] [PubMed]

25. Cheng, Z.; Liu, W.; Fan, R.; Han, S.; Li, Y.; Cui, X.; Zhang, J.; Wu, Y.; Lv, X.; Zhang, Y.; et al. Terpenoids from the deep-sea-derived fungus *Penicillium thomii* YPGA3 and their bioactivities. *Mar. Drugs* **2020**, *18*, 164. [CrossRef] [PubMed]

26. Qiu, P.; Liu, Z.; Chen, Y.; Cai, R.; Chen, G.; She, Z. Secondary metabolites with α-glucosidase inhibitory activity from the mangrove fungus *Mycosphaerella* sp. SYSU-DZG01. *Mar. Drugs* **2019**, *17*, 483. [CrossRef]

27. *Sybyl Software*, Version X 2.0; Tripos Associates Inc.: St. Louis, MO, USA, 2013.

28. Frisch, M.J.; Trucks, G.W.; Schlegel, H.B.; Scuseria, G.E.; Robb, M.A.; Cheeseman, J.R.; Scalmani, G.; Barone, V.; Mennucci, B.; Petersson, G.A.; et al. *Gaussian 09, Rev. C 01*; Gaussian, Inc.: Wallingford, CT, USA, 2009.

29. Stephens, P.J.; Harada, N. ECD cotton effect approximated by the Gaussian curve and other methods. *Chirality* **2010**, *22*, 229–233. [CrossRef] [PubMed]